Horticultural Plant Journal

Available online at www.sciencedirect.com
The journal's homepage: http://www.keaipublishing.com/en/journals/horticultural-plant-journal

Research Paper

Expression changes of miRNA-regulated genes associated with the formation of the leafy head in cabbage

Jorge Alemán-Báez, Jose Fernando Acevedo-Zamora, Johan Bucher, Chengcheng Cai, Roeland E. Voorrips, and Guusje Bonnema *

Plant Breeding, Wageningen University and Research, Wageningen, The Netherlands

Received 30 March 2023; Received in revised form 23 June 2023; Accepted 13 August 2023

Available online 16 March 2024

A B S T R A C T

The vegetative development of cabbage (*Brassica oleracea* var. *capitata*) passes through seedling, rosette, folding and heading stages. Leaves that form the rosette are large and mostly flat. In the following developmental stages, the plants produce leaves that curve inward to produce the leafy head. Many microRNAs and their target genes have been described participating in leaf development and leaf curvature. The aim of this study is to investigate the role of miRNA-regulated genes in the transition from the rosette to the heading stage. We compared the miRNA and gene abundances between emerging rosette and heading leaves. To remove transcripts (miRNAs and genes) whose regulation was most likely associated with plant age rather than the change from rosette to heading stage, we utilized a non-heading collard green (*B. oleracea* var. *acephala*) morphotype as control. This resulted in 33 DEMs and 1 998 DEGs with likely roles in the transition from rosette to heading stage in cabbage. Among these 1 998 DEGs, we found enriched GO terms related to DNA-binding transcription factor activity, transcription regulator activity, iron ion binding, and photosynthesis. We predicted the target genes of these 33 DEMs and focused on the subset that was differentially expressed (1 998 DEGs) between rosette and heading stage leaves to construct miRNA-target gene interaction networks. Our main finding is a role for miR396b-5p targeting two *Arabidopsis thaliana* orthologues of *GROWTH REGULATING FACTORs 3* (*GRF3*) and 4 (*GRF4*) in pointed cabbage head formation.

Keywords: *Brassica oleracea* var. *capitata*; RNA sequencing; miRNA-target gene network; leafy head formation

1. Introduction

Cabbage (*Brassica oleracea* var. *capitata*) is an important vegetable crop consumed worldwide. The edible and economically important part of cabbage plants is the leafy head. Cabbage plants undergo four vegetative stages: seedling, rosette, folding, and heading. Seedling leaves are mostly flat, have clear petioles, and remain relatively small. Rosette leaves are mostly flat and are the largest leaves of the cabbage plant. Folding leaves are curved upwards and inwards. Heading leaves show an extreme inward curvature that causes their overlapping around the shoot apical meristem (SAM) to produce the leafy head. These leaves are not exposed to light and therefore do not photosynthesize; instead, they serve as storage organs. In cabbage, the molecular pathways that control the morphological changes from flat rosette leaves to curved heading leaves remain unclear. Interestingly, studies in *Arabidopsis thaliana* (Liu et al., 2011; Kalve et al., 2014; Yang et al., 2018) and the heading Chinese cabbage (*Brassica rapa* ssp. *pekinensis*) (Mao et al., 2014; Li et al., 2019) show the essential participation of microRNAs (miRNAs) and their target genes in leaf development and leaf curvature.

Many miRNAs families are very conserved among the plant kingdom (Zhang et al., 2006), and are involved in many biological processes such as growth, development, hormone signalling, and abiotic/biotic stress responses (Dong et al., 2022; Islam et al., 2022;

* Corresponding author.
E-mail address: guusje.bonnema@wur.nl

Peer review under responsibility of Chinese Society of Horticultural Science (CSHS) and Institute of Vegetables and Flowers (IVF), Chinese Academy of Agricultural Sciences (CAAS)

https://doi.org/10.1016/j.hpj.2023.08.002

Kumar et al., 2022; Zhang et al., 2022; Zhu et al., 2022). Many miRNAs are involved in leaf initiation and development. Studies in *Arabidopsis thaliana* (Palatnik et al., 2003; Williams et al., 2005; Song et al., 2012) and Chinese cabbage (Ren et al., 2018) showed that changes in the miRNA-target gene interactions related to leaf development can affect the morphology of leaves such as their size, curvature, or margins. The leaf primordia originate from the peripheral zone in the shoot apical meristem (SAM) where miR394 negatively regulates the LEAF CURLING RESPONSIVENESS (LCR) protein (Knauer et al., 2013). LCR interferes with the interaction between gene products of homeodomain transcription factor (TF) WUSCHEL (WUS) and CLAVATA (CLV1 and CLV2), which is an important factor in stem cell maintenance. Song et al. (2012) overexpressed, in *A. thaliana*, a version of *LCR* not regulated by miR394, which resulted in downward curved leaves. In contrast, the overexpression of miR394 produced upward curved leaves. After leaf primordia initiation, the adaxial–abaxial, the proximal-distal, and the medial-lateral polarities are established. During the ad/abaxial polarity establishment, the adaxial domain is determined by a group of plant-specific homeodomain/leucine zipper (HD-ZIP) transcription factors (TFs), which are positively regulated by ASYMMETRIC LEAVES AS1 and AS2 (Yang et al., 2018) and negatively regulated by miR165/166 (Kim et al., 2005). The overexpression of miR166g in *A. thaliana* produced downward curving leaves (Williams et al., 2005). Similarly, the overexpression of miR166g in Chinese cabbage caused rosette leaves to change from flat into downward curving, folding leaves to change from upward curving into flat, and the production of smaller leafy heads when compared to non-mutated plants (Ren et al., 2018). Meanwhile, the abaxial domain is determined by the YABBY (YAB) TFs family, which are activated by KANADI (KAN) TFs and *AUXIN RESPONSE FACTORS 3* and *4* (*ARF3/4*) (Chitwood et al., 2007, 2009; Yamaguchi et al., 2012). *ARF3* and *ARF4* are negatively regulated by miR390-derived transacting small interfering RNAs (tasiRNA) (Allen et al., 2005). During cell proliferation, miR319/JAW negatively regulates the expression of members of the *TEOSINTE BRANCHED/ CYCLOIDEA/PCF* (*TCP*) genes (Palatnik et al., 2003) which are involved in controlling cell division and cell expansion to maintain the flatness (shape) of leaves (Nath et al., 2003). The overexpression of miR319/JAW in *A. thaliana* produced serrated and curved leaves (Palatnik et al., 2003). In Chinese cabbage, the overexpression of miR319a produced rosette leaves with wavy margins and changed the leafy head shape from round to cylindrical (Mao et al., 2014). TCP TFs promote the expression of miR164 (Koyama et al., 2010) and miR396 (Schommer et al., 2014), which have opposing functions in leaf cell proliferation: miR164 targets *CUP-SHAPEDCOTYLEDON* (*CUC*) genes, which negatively regulate cell proliferation (Raman et al., 2008), whereas miR396 targets *GRF-INTERACTING FACTOR1* (*GF1*) genes, which promotes cell proliferation and controls the final number of cells in leaves (Debernardi et al., 2014). The overexpression of miR396 in *A. thaliana* lowered the *GRF* levels, resulting in reduced cell proliferation and smaller leaves (Rodriguez et al., 2010).

Additionally, variations in the miRNA-target gene interactions were shown to be involved in the plant age (general development) and the timing of the phase transition from juvenile to adult. In *A. thaliana*, miR156 targets SPL (SQUAMOSA-promoter binding protein-like) transcription factors, which play essential roles in plant growth and development and are well known to regulate the transition of leaves from juvenile to adult stage (Wu and Poethig, 2006, 2009; Preston and Hileman, 2013). In Chinese cabbage, the overexpression of *SPL9-2* shortened the seedling and rosette stage and accelerated the heading process while the overexpression of miR156 delayed the folding of leaves (Wang et al., 2014).

Next-generation sequencing (NGS) is a powerful and accurate technology to identify small RNA (sRNA) and messenger RNA (mRNA) transcripts and estimate their abundance. This technology has been utilized in cabbage (Zhang et al., 2022) and Chinese cabbage (Wang et al., 2012, 2012b, 2013; Gu et al., 2017; Zhang et al., 2022) to identify differentially expressed miRNAs (DEMs) or genes (DEGs) putatively involved in the leafy head formation process. This resulted in the identification of DEMs like miR399, miR1521, miR2630, and miR3631 (Wang et al., 2013) and DEGs with significantly enriched gene ontology (GO) terms like hormone (auxin and abscisic acid) signalling (Gu et al., 2017; Sun et al., 2019), photosynthesis (Sun et al., 2019; Zhang et al., 2022), carbohydrate metabolism (Wang et al., 2012; Zhang et al., 2022), DNA replication (Zhang et al., 2022), transcription regulator activity (Wang et al., 2012; Zhang et al., 2022) and cytoskeleton proteins (Wang et al., 2012; Zhang et al., 2022). Interestingly, Zhang et al. (2022) showed that the heading transition was independent from the developmental phase transition (juvenile to adult: aging). Far fewer studies exist that investigate the leafy head formation in cabbage (*B. oleracea*) than in Chinese cabbage (*B. rapa*). Zhang et al. (2022) however compared the transcriptome changes during development from rosette to heading stage of Chinese cabbage with those in cabbage. One clear difference was that in the transition stage of Chinese cabbage the ethylene pathways were highly activated, which was not the case during cabbage transition to the heading stage, illustrating differences in leafy head development between *B. rapa* and *B. oleracea*.

Our aim in this study is to understand the involvement of miRNA-regulated genes in cabbage leafy head formation by using an integrated analysis of DEMs with DEGs, focusing on the transition from flat rosette to incurved heading leaves. To achieve this, we phenotyped leaf initiation and expansion throughout plant development to determine the rosette and heading stages for both a pointed and round cabbage morphotype. Additionally, we determined the equivalent of these cabbage stages for a non-heading collard green (*B. oleracea* var. *acephala*) cultivar. For the three morphotype specific developmental stages, we performed RNA sequencing of young leaves destined to develop into rosette and heading leaves to estimate the miRNA and mRNA abundance. We compared the transcript abundance of both heading cabbages with the non-heading collard to identify DEMs and DEGs putatively involved in the transition from rosette to the leafy head stage. To identify the miRNA-gene interactions, we integrated the abundance of DEMs with DEGs using miRNA target prediction tools and correlation analysis. Our study provides new insights into the regulatory network controlling the leafy head formation in cabbage.

2. Material and Methods

2.1. Plant material

Three *B. oleracea* hybrid cultivars were utilized in this study: a pointed heading cabbage ('Sonsma', breeding company "Rijk Zwaan Zaadteelt en Zaadhandel B.V., De Lier, The Netherlands"), a round heading cabbage ('Excalibur', breeding company "Bejo Zaden, Warmenhuizen, The Netherlands"), and a non-heading collard green ('Teddy', Chiltern Seeds, Wallingford, England). The two cabbage morphotypes were selected for their contrasting leafy head shape and the collard morphotype for its close phylogenetic relationship with the heading cabbages (Cai et al., 2022). Seeds from these morphotypes were sown in germination trays with sandy soil in the Unifarm greenhouse at Wageningen University & Research (51°59′11″N latitude, 05°39′52″E longitude) during the last week of August 2020. The seedlings were cultured in a greenhouse (16 h/8 h day/night cycle, temperature 23.1 °C (on average), relative humidity 60% (on average). Twelve days after sowing (DAS), the seedlings were transplanted into two liter pots with potting compost (Lentse potgrond No.2) and placed within the same greenhouse following a Randomized Complete Block Design (RCBD) with three blocks. Each of these blocks served as a biological replicate. Each block included one plot of 20 plants of each *B. oleracea* morphotype.

2.2. Collection of leaf tissue

Leaf tissue samples were collected from each morphotype at nine time points: 28, 35, 42, 49, 56, 63, 70, 77, and 84 days after sowing (DAS). The leaf tissue collection occurred always between 14:00 and 15:30 (Central European Time). At each time point, two plants from each morphotype, within the same block, were selected randomly and leaf tissue from the smallest leaf $\geq$ 1.5 cm of each plant was collected and pooled into a single sample. All leaf tissue samples included only the right portion of the leaf lamina (proximo-distal perspective) excluding the main vein. After collection, the leaf samples were quickly frozen with liquid nitrogen and stored at −80 °C for the extraction of total RNA.

2.3. Phenotyping of leaf development

At each time point, one of the two plants per block of each morphotype previously utilized for sampling leaf tissue was randomly selected for phenotyping. This resulted in phenotyping three plants of each morphotype at each time point. For each of these plants, the total number of leaves was counted, including the scars on the stem produced by leaves that had dropped from the plant. For both cabbage morphotypes, the leaf position (from the oldest to the youngest) of the first heading leaf was scored. This was defined as the oldest (outermost) leaf that was part of the leafy head. For all three morphotypes, the complete set of leaves (including small inner heading leaves) of each plant was detached from the stem and counted. Only leaves of sufficient size (length $\geq$ 4 cm) were selected for further morphological analysis using ImageJ software (Schneider et al., 2012). These selected leaves were positioned from oldest to youngest, photographed (Fig. S1), and used to extract measurements such as leaf area, height, and width (at the widest point) (Fig. S1) every single leaf.

2.4. Small RNA and messenger RNA libraries construction and sequencing

Total RNA was isolated, respectively, from the leaf tissue samples using TRIzol reagent (Invitrogen, USA) according to the manufacturer's protocol. The quality of the RNA samples was checked for purity ($OD_{260/280} \geq 2.0$ and $OD_{260/230} \geq 2.0$) and integrity (RIN $\geq$ 7.0). In total, 18 RNA samples (two developmental stages, three *B. oleracea* morphotypes, three biological replicates) were shipped to Novogene (UK) for library construction and sequencing. The total RNA of each sample was utilized to construct two libraries: one with small RNAs and one with messenger RNAs. Small RNA libraries were constructed using the TruSeq Small RNA Library Preparation Kit (Illumina, United States). Single-end sequencing was performed to produce reads $\leq$ 50 bp using the Illumina NovaSeq 6000 platform (Illumina, United States). Messenger RNA libraries were purified using Dynabeads™ Oligo (dT) (Thermo Fisher, United States) and the ribosomal RNA (rRNA) was removed using the Ribo-Zero kit (Illumina, United States). Paired-end sequencing was performed to produce 150 bp reads with an insert size of 250—300 bp using the Illumina NovaSeq 6000 system (Illumina, United States). Table S1 shows the adaptor sequences utilized, respectively, in the sequencing of the sRNA and mRNA libraries. A pre-filtering process was performed for both sRNA and mRNA libraries to remove reads with low quality. For this, sRNA and mRNA reads where $\geq$ 50% of the bases have a quality score (Qscore) $\leq$ 5 and/or that contain > 10% of uncertain nucleotides (N) were removed. Raw sRNA and mRNA sequencing data can be found in the NCBI Sequence Read Archive under the accession number PRJNA110106.

2.5. Small RNA analysis

For each sRNA library, we retained reads with lengths ranging from 18 to 30 nucleotides (nt), which are referred as "clean reads". To identify the unique clean reads within each sRNA library and quantify their occurrence, the "collapse reads" module of miRDeep2 v0.1.3 software (Friedländer et al., 2012) was utilized with default parameters. From these, the unique clean sequences occurring only once were removed from further analyses. To identify the clean reads present in all biological replicates, the command "common" from the SeqKit v2.2.0 (Shen et al., 2016) tool was used with default parameters. These common reads were mapped to the JZS v2 (Cai et al., 2020) cabbage reference genome using Bowtie2 v2.4.4 (Langmead and Salzberg, 2012) software with default parameters (allowing no mismatches) to determine their overall alignment. To identify the reads annotated as non-miRNAs (like rRNA, tRNA, snRNA, snoRNA) among the sRNA libraries, the command "cmscan" (parameters: oskip, oclan, nohmmonly, rfam, and fmt=2) from Infernal v1.1.4 (Nawrocki and Eddy, 2013) was used, where the non-miRNAs sequences were obtained from the Rfam database (https://rfam.xfam.org/; accessed 15 September 2021).

2.6. Identification of known miRNAs

The sRNA libraries include reads 18—30 bp long and only part of these are miRNAs. To identify known miRNAs among the sRNA libraries, the "quantifier" module of miRDeep2 v0.1.3 software was utilized with default parameters (which allows max one

mismatch). With this algorithm, the known miRNA sequences of all plants (including members of the Brassicaceae family) deposited in the miRBase 22.1 database (http://www.mirbase.org/ ; accessed 29 September 2021) were mapped to the miRNA hairpin precursor sequences of members of the Brassicaceae family also deposited in the miRBase 22.1 database (accessed 29 September 2021). The Brassicaceae hairpin precursors to which any known miRNA mapped were selected. All the reads included in each sRNA library were mapped (allowing one mismatch) to these miRNA hairpin precursor sequences. The number of reads that completely aligned to an interval 2 nt upstream and 5 nt downstream where the sequence of a known miRNA aligned were quantified and considered as raw counts for the respectively known miRNA.

2.7. mRNA analysis

The raw mRNA paired-end reads were filtered to obtain high-quality reads using Trimmomatic −0.39 (Bolger et al., 2014) with ILLUMINACLIP = TruSeq3-PE.fa:2:30:10:2, LEADING = 3, TRAILING =3 and MINLEN = 36 as parameters. These high-quality paired-end reads were aligned to the JZS v2 (Cai et al., 2020) reference genome utilizing the HISTAT2 2.1.0 (Kim et al., 2019) software with parameters "−dta -no-softclip". We then utilized StringTie 2.1.4. (Pertea et al., 2015) software with −e and −G as parameters to compute the expression level of each annotated gene in terms of transcripts per kilobase of exon model per million mapped reads (TPM).

2.8. Analysis of miRNAs and gene expression levels

The analysis of sRNAs and mRNAs allowed us to identify and quantify the abundance of known miRNAs and gene transcripts in pointed cabbage, round cabbage, and collard green plants at rosette/stage-one and heading/stage-two developmental stages. We refer to the abundance of a transcript as the expression of a transcript. To enable an accurate comparison between the sRNA and mRNA libraries, the size of each library was adjusted (normalized) using the "calcNormFactors" function from the edgeR 3.34.1 (Robinson et al., 2010) package by applying the Trimmed Mean of M-values (TMM) method (Robinson and Oshlack, 2010). This method applies a linear scaling factor to each library based on a weighted mean of log ratios between each library and a reference library (which has the closest average expression to the mean of all libraries). After applying this library adjustment, the expression levels of all miRNAs/genes are presented as counts per million (CPM) and transcripts with a low expression of < 3 CPM were removed. This threshold was determined based on Sha et al. (2015). To filter against transcripts with low expression, we calculated for each transcript the average count over the biological replicates (morphotype − developmental stage combination). If more than one of the replicates had zero counts of a transcript, that transcript was considered not to be present in that morphotype at that stage. If the average count of a transcript over all six morphotypes/stage combinations was < 3 CPM, the transcript was considered as not expressed. To estimate the dispersion between libraries based on their transcripts (miRNAs/genes) expression, the "estimateDisp" function from the edgeR 3.34.1 (Robinson et al., 2010) package was utilized with default parameters. To visualize these dispersion estimates on a scatterplot, the function "plotMDS" of the limma 3.48.3 (Ritchie et al., 2015) package was used.

2.9. Differential expression analysis of miRNAs and genes between B. oleracea tissues

The main aim of this study is to identify the transcripts (miRNAs and genes) involved in the leafy head formation in round and pointed cabbage. To achieve this, five contrast were created to compare the expression of transcripts between the six tissue samples (Table 1). Contrast-SR (for Stage in Round cabbage) and -SP (for Stage in Pointed cabbage) identifies differentially expressed (DE) transcripts in leaf tissue samples collected from the same cabbage morphotype at different developmental stages, while contrast-SC (for Stage in Collard) identifies DE in collard leaves of different ages. Moreover, contrast-DR (for Development, Round cabbage) and -DP (for Development, Pointed cabbage) subtract contrast-SC (age) from contrast-SR and -SP (developmental stages). Contrast-SR, -SP, and -SC were analyzed with the "glmQLFTest" function of the edgeR 3.34.1 (Robinson et al., 2010) package which conducts a miRNA-/genewise statistical *t*-test for each contrast. Based on Ye et al. (2016), a criterion of $|\log_2 FC| \geq 1$ and *p*. adjusted value < 0.05 were set as the threshold for statistically significant differential expression. To control the problem of false discovery rate produced by multiple testing, the *p*.value from each statistical test was adjusted using the "BH" method (Benjamini and Hochberg, 1995).

2.10. Gene ontology annotation

To identify the biological functions of the DEGs, we retrieved the gene ontology (GO) terms for these genes using the TBtools v1.098746 (Chen et al., 2020) software. For this, the InterPro gene annotations of the JZS v2 genome obtained from the BRAD database (http://brassicadb.cn/; accessed 28 March 2022) were converted into Gene Ontology (GO) terms using the "interpro2go"

Table 1 Differentially expressed known miRNAs and genes among the five contrasts

Contrast	Known miRNAs			Genes		
	Down	Not Sig	Up	Down	Not Sig	Up
Contrast-SR = Round (HS) − Round (RS)	15	84	12	911	31 074	423
Contrast-SP = Pointed (HS) − Pointed (RS)	37	72	2	1 022	30 714	672
Contrast-SC = Collard (S2) − Collard (S1)	10	91	10	375	31 908	125
Contrast-DR = Contrast-SR − Contrast-SC	6	99	6	600	31 482	326
Contrast-DP = Contrast-SP − Contrast-SC	23	86	2	802	31 008	598

Note: RS = Rosette stage; HS = Heading stage; S1 = Stage-one; S2 = Stage-two. Contrast-SR, -SP, -SC = contrasts between Stages in Round and Pointed cabbage and in Collards; Contrast-DR and -DP = Development-specific contrasts in Round and Pointed cabbage. Down = Downregulated; Not Sig = Not significantly differentially expressed; Up = Upregulated.

annotation file obtained from the InterPro database (https://www.ebi.ac.uk/interpro/download//; accessed 28 March 2022).

2.11. Prediction of miRNAs targets

To predict the miRNA target genes, the miRNA sequences were aligned to the coding DNA sequences of the JZS v2 genome (http://brassicadb.cn/; accessed 22 July 2021) using both miRanda (Enright et al., 2003) and RNAhybrid (Rehmsmeier et al., 2004) software. The parameters utilized in these software were based on Zhang and Verbeek (2010). These parameters were: a minimum free energy threshold of −18.0 kcal · mol^{-1}, and no adjacent mismatches in positions 2–7 of the miRNA/target duplex. To visualize in a heatmap (including a dendrogram) the hierarchical clustering of the mRNA libraries based on the expression of these predicted targeted genes, the R "heatmap" function of the stats v4.1.0 package (R Core Team, 2022) and the genes expression values in log2 scale were utilized.

2.12. Correlation analysis of the abundance of miRNAs and mRNAs

To identify miRNAs significantly negatively correlated to genes, the expression levels of these transcripts among the six leaf tissue samples collected from the three *B. oleracea* morphotypes were analyzed by the Pearson correlation method included in the R "cor.test" function from the stats v4.1.0 package (R Core Team, 2022). To visualize these correlations in scatter plots, the R "geom_point" and "geom_smooth" function from the ggplot2 v3.3.5 package (Wickham, 2016) was utilized. Moreover, these negative correlations were utilized to construct the miRNA-target gene regulatory network using Cytoscape v3.9.1 (Franz et al., 2016) software. The *Arabidopsis* Information Resource (TAIR) database (http://arabidopsis.org, accessed 31 May 2022) was utilized to annotate the cabbage (*B. oleracea*) orthologous genes in *A. thaliana*.

3. Results

3.1. Establishment of developmental stages in cabbage and collard plants

At weekly intervals from 28 to 84 DAS, all the leaves of three plants from each of the three *B. oleracea* morphotypes (pointed cabbage, round cabbage, and collard green) were counted and photographed. This provided information concerning the time intervals between the formation of each leaf. We determined the size of each leaf at these weekly harvests, to get information of both the growth speed and the final size of each leaf (Figs. S2, S3, and S4). Fig.1, A shows the three *B. oleracea* morphotypes at 77 DAS when both pointed and round cabbages had formed a leafy head and Fig. 1, B shows all their leaf sizes. Based on these combined data (growth speed and size), we could identify the rosette leaves (Fig. 1, A, B), which are defined as those leaves that reach the largest area, length, and width from the complete set of leaves included in a cabbage plant. At 77 DAS, the rosette leaves were at positions 7—14 (from oldest to youngest) in pointed cabbage plants and positions 8—16 in round cabbages (Fig. 1, A, B; Figs. S2 and S3). The pointed cabbage plants produced most of these leaves between 35—49 DAS and round cabbage between 42—56 DAS (Fig. 1, C; Table S2). These DAS are defined as the rosette stage (in cabbages). As the leaf production rate of collard plants was very similar to that in round cabbage plants (Fig. 1, C; Table S2), we defined collard "stage-one" also as 42—56 DAS and defined it as the equivalent of the rosette stage in cabbage.

To determine the start of the heading stage in both cabbages, the position of the first heading leaf (outer leaf surrounding the leafy head) observed at 77 DAS was used (Table S3). For pointed cabbages, the first heading leaf was, on average, leaf 21 and for round cabbages leaf 24 (Table S3). These leaves were, approximately, produced at 56 DAS in pointed cabbages and 70 DAS in round cabbages (Fig.1, C; Table S2). These time points are determined as the start of the heading stage. For the non-heading collard plants, the "stage-two", which is the equivalent of the heading stage in cabbages, was also set at 70 DAS as for round cabbages. This was again based on the similar leaf production rate (Fig.1, C; Table S2) between round cabbages and collard green plants. Fig. 1, A clearly shows the curvature of heading leaves in both round and pointed cabbages and the flat/wavy "stage-two" leaves in collard plants.

3.2. Small RNA reads from cabbages and collard show a similar overall alignment to a cabbage reference genome

For sRNA and RNA sequencing, rosette leaf tissue was sampled at the midpoint of rosette stage (at 42 DAS for pointed and at 49 DAS for round) in both cabbage genotypes and at 49 DAS as "stage-one" in collard plants. For both cabbage genotypes heading leaf tissue was sampled seven days after the start of the heading stage (at 63 DAS for pointed and at 77 for round). For collard "stage-two" leaf tissue was sampled at 77 DAS (like for round heading leaf tissue).

The young leaf tissue samples yielded 18 sRNA libraries (three *B. oleracea* morphotypes, two developmental stages, collected in triplicate). On average, these 18 sRNA libraries contained 25.1 million (M) of raw reads (Table S4) of which, on average, 20.4 M were "clean reads" (Tables S4 and S5). A sRNA library constructed from one replicate of the rosette leaf tissue collected from round cabbages (Round.RS.1) contained a relatively low number of clean reads (Fig. 5; Table S5). For this reason, we removed this sRNA library from further analysis. Since the sRNAs involved in the leafy head formation should be expressed consistently between biological replicates, we focus only on those commonly detected between all biological replicates. On average, 655.6 thousand (K) unique clean reads were "common" between biological replicates (Table S5). There was no difference in the matching of these common reads from both cabbages (78.0%) and the collard (78.2%) to the JZS v2 reference genome (Table S6). On average, 30.2 K (4.7%) of the common reads (Table S7) were annotated as non-miRNAs and removed from further analysis.

3.3. MiRNA expression between pointed and round cabbage is similar at their rosette stages yet differs between both heading stages

The interactions between miRNAs and their target genes play a crucial role in the development of leaf curvature, which is essential for the formation of the leafy head. To identify the specific miRNAs involved in the leafy head formation, we annotated the "common"

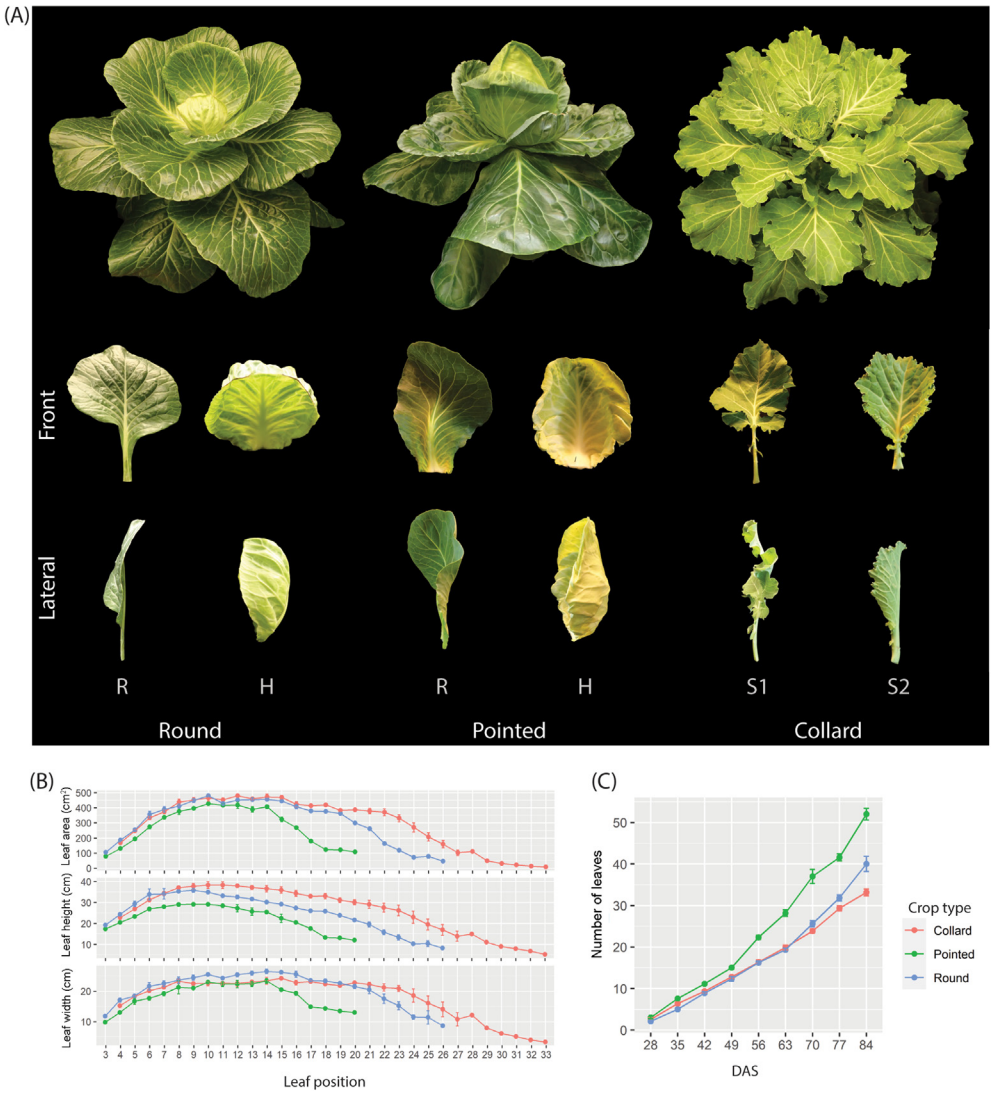

Fig. 1 Determination of developmental stages in cabbage and collard plants

(A) Upper part and from left to right: round cabbage, pointed cabbage, and collard green plants at 77 Days After Sowing (DAS); lower part and from left to right: front and lateral perspective of rosette (R) and heading (H) leaves in round and pointed cabbages and of "stage-one" (S1) and "stage-two" (S2) in collard. (B) Area (cm^2), height (cm), and width (cm) of mostly non-heading (seedling, rosette and folding) leaves of the three *B. oleracea* morphotypes at 77 DAS. (C) Total number of leaves (length > 1 cm) of the three *B. oleracea* morphotypes at different DAS.

reads as miRNAs. In total, 111 conserved miRNAs, belonging to 43 miRNA families, were detected among the 17 sRNA libraries (Tables S8 and S9). The expression of these conserved miRNAs was normalized by applying a scaling factor (Table S10) to each sRNA library. These adjusted values (in CPM) (Table S11) were utilized in all downstream analyses. From these 111 conserved miRNAs, 88 were commonly expressed among the three *B. oleracea* morphotypes, three were only expressed in pointed cabbage at rosette stage (miR156c-3p, miR156g-3p, and miR9557-3p), one only in round cabbage at rosette stage (miR156a-3p) and two only in collard (miR400-5p in S1 and miR9568-5p in S2) (Fig. 2, A; Table S9). The miR159, miR162, miR165, miR166, and miR168 families, which were expressed in all three *B. oleracea* morphotypes, included the most highly expressed miRNAs with an expression over 100 k CPM (Fig. 2, B; Table S11).

The multidimensional scaling (MDS) plots show the dispersion of the 17 sRNA libraries based on the expression levels of conserved miRNAs (Fig. 2, C). In this plot, the biological replicates of each morphotype/developmental stage leaf sample cluster together. Interestingly, the leaf samples collected from both cabbage morphotypes at rosette stage cluster together. This is clearly not the case for both cabbage tissue samples collected at heading stage.

3.4. *Messenger RNA expression in pointed and round cabbages is very similar between rosette- and heading-stages*

Like for the small RNA libraries, 18 mRNA libraries were also constructed from the three *B. oleracea* morphotypes (pointed cabbage, round cabbage, and collard) at two developmental

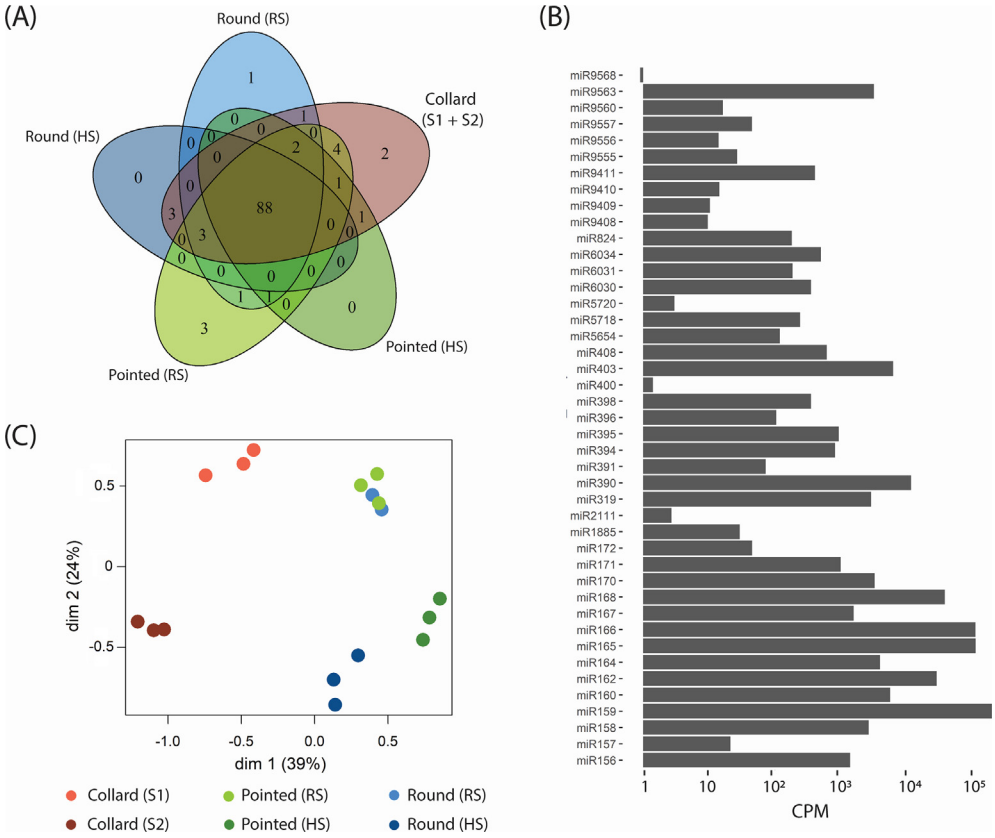

Fig. 2 Summary of conserved miRNAs identified in three *B. oleracea* morphotypes (round and pointed cabbage and collard)
(A) Venn diagram of the expression of known miRNAs in the six tissue samples. (B) Expression (in counts per million of transcripts) of the conserved miRNA families. (C) MDS plot (explained variance for dim1 = 39%; dim2 = 24%) of the 17 sRNA libraries based on the expression levels of conserved miRNAs. RS=rosette stage, HS=heading stage in the two cabbage morphotypes, S1 (Stage-one) and S2 (Stage-two) are stages of collard corresponding to these stages.

stages (rosette/stage-one and heading/stage-two) in triplicate. For the analysis of mRNAs, we removed the same biological replicate that was also removed from the sRNA analysis due to a low number of high-quality reads (Results 3.2 and Fig. S5). On average, the remaining 17 mRNA libraries contain 22.4 M raw read pairs (44.8 M paired-end reads) of which, on average, 21.2 M are high-quality read pairs (Table S12). Like for the sRNA libraries, the mRNA libraries from both cabbages (90.0%) and collard (90.2%) show a similar overall alignment to the JZS v2 (Cai et al., 2020) cabbage genome (Table S13). These aligned reads were compared to the JZS v2 CDS to estimate the raw gene expression (Table S14) and by applying a scaling factor (Table S10) to each mRNA library, the adjusted gene expression values (Table S15) were obtained. In total, 32 408 genes of the 59 064 JZS v2 (Cai et al., 2020) predicted genes were expressed in at least one of the six morphotype/development leaf samples (Table S15). Of these 32 408 genes, 30 532 are expressed in all three morphotypes, 175, 176, and 223 genes are only expressed in respectively pointed cabbage, round cabbage, and collard (Fig. 3, A; Table S15). Moreover, within a *B. oleracea* morphotype, the number of expressed genes varies among developmental stages (Fig. 3, B). Fig. S6 shows the dispersion of the 17 libraries based on the expression levels of *B. oleracea* genes. Unlike the dispersion produced by the conserved miRNAs (Fig. 2, C), both the biological repeats and the developmental stages collected from the same *B. oleracea* morphotype cluster tightly together.

3.5. *Non-heading Collard control assigns 40% of DEMs and 20% DEGs between rosette and heading stages of cabbage to the aging pathway*

To identify DEMs and DEGs putatively related to the leafy head formation, we utilized five contrasts (Table 1). For the differential expression analysis of miRNAs, first we compared the transcript abundance between leaves of the rosette and heading Stages of Round (contrast-SR) and Pointed (contrast-SP) cabbages. These two contrasts (-SR and -SP) identified, in total, 53 DEMs from 21 miRNA families (Table 1, Fig. S7, A, Table S16). Among these 53 DEMs, more miRNAs had lower transcript abundance in heading stage vs. rosette stage than vice versa in both round and pointed cabbages (Table 1 and Table S16). Additionally, more DEMs were identified in the pointed cabbage (39, contrast-SP) than in round cabbage (27, contrast-SR). Twenty of these 53 DEMs were also differentially expressed between leaves of the "stage-one" and "stage-two" of collard (contrast-SC; Table 1, Fig. S7, A and Table S16). We are especially interested in the miRNAs and mRNAs that play a role in the development from the rosette to heading stage of cabbages, but not in those that are involved in aging. We

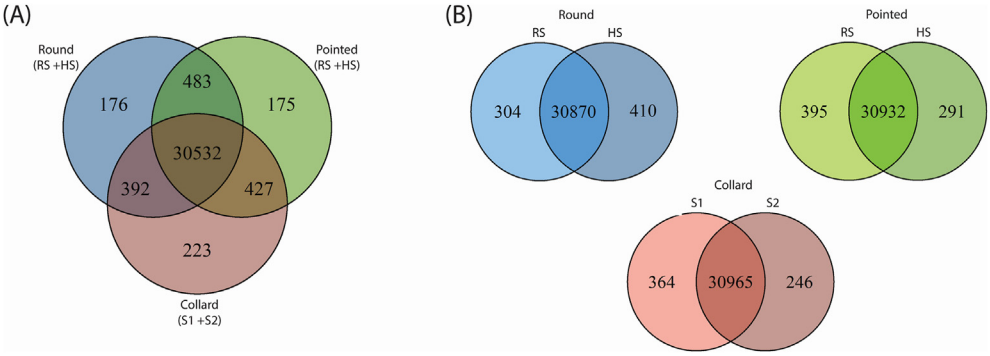

Fig. 3 Venn diagrams of the number of genes expressed in three *B. oleracea* morphotypes (round and pointed cabbage and collard)
(A) The total number of genes expressed in the three *B. oleracea* morphotypes. (B) The number of genes expressed in each of the three *B. oleracea* morphotypes at two developmental stages. RS = rosette stage, HS = heading stage in the two cabbage morphotypes, S1 (Stage-one) and S2 (Stage-two) are stages of collard corresponding to these stages.

assume that those 20 DEMs between leaves of the "stage-one" and "stage-two" of collard (Contrast-SC; Stage Collard) are mostly in this aging category; therefore, to obtain the DEMs involved in the Development we subtract those 20 DEMs from the 53 DEMs identified in the round (contrast-SR) and pointed (contrast-SP) cabbage morphotypes. In total, 33 unique DEMs were identified to be involved in the Development from the rosette to heading stage in Pointed (contrast-DP) and Round (contrast-DR) cabbage morphotypes (Table 1, Fig. S7, A, and Table S16). From these 33 DEMs, 8 miRNAs were identified only in round cabbage (contrast-DR), 21 miRNAs only in pointed cabbage (contrast-DP), and four miRNAs (miR5718, miR6034, miR9408, and miR9555a-5p) in both cabbages (Table 1, Fig. S7, A and Table S16). Members of miRNA families miR156, miR171, miR172, miR398, and miR1885 were only identified in round cabbage (contrast-DR) whereas members of miRNA families miR164, miR395, miR396, miR2111, miR5456, miR9409, and miR9557 were only identified in pointed cabbage (contrast-DP) (Table S16).

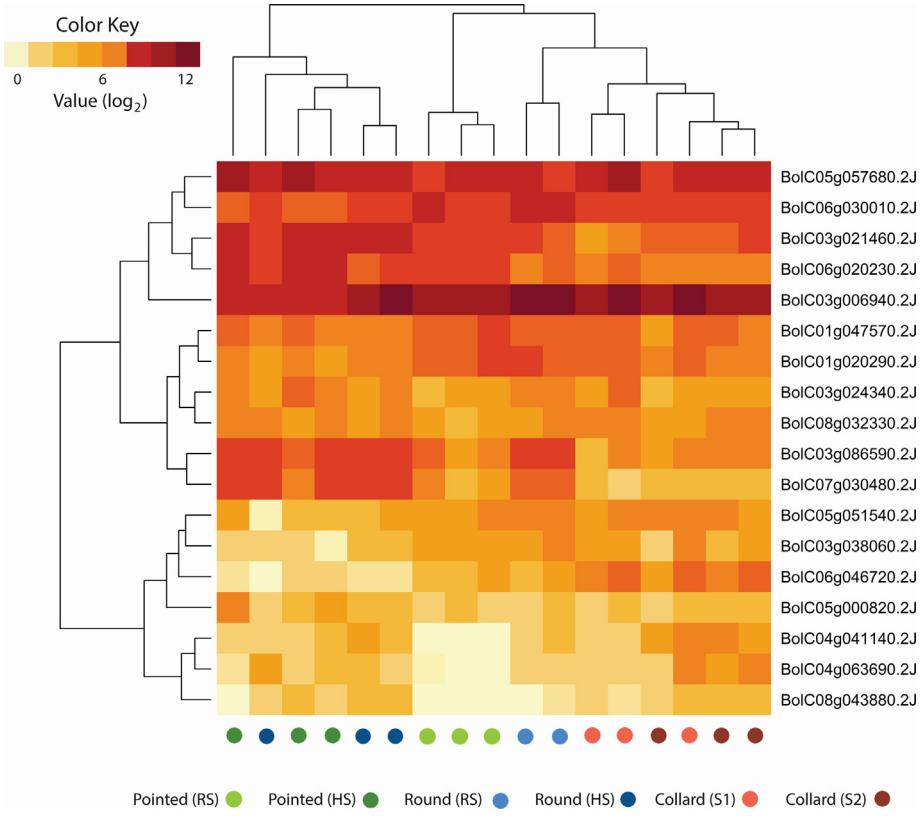

Fig. 4 Heatmap of the 17 mRNA libraries based on the expression of 18 DEGs putatively targeted by DEMs
RS=rosette stage, HS=heading stage in the two cabbage morphotypes, S1 (Stage-one) and S2 (Stage-two) are stages of collard corresponding to these stages.

For the differential expression analysis of genes, we followed the same methodology as for the differential expression analysis of miRNAs. In total, 2 498 DEGs were identified between the leaves of the rosette and heading Stages of Round (contrast-SR) and Pointed (contrast-SP) cabbages (Table 1, Fig. S7, B, and Table S17). Like in the DEMs analysis, more genes had lower transcript abundance in heading stage compared to rosette stage in both cabbages, and more DEGs were identified in the pointed cabbage (1 694; contrast-SP) than in round cabbage (1 334; contrast-SR) (Table 1, Fig. S7, B and Table S17). Out of the 2 498 DEGs (contrast-SP and contrast-SR), 500 were differentially expressed between leaves of the "stage-one" and "stage-two" of collard (contrast-SC; Table 1, Fig. S7, B and Table S17). These 500 DEGs (contrast-SC) are assumed to be involved in the plant aging rather than in the development from the rosette to heading stage in cabbages. In total, 1 998 DEGs were identified in round (contrast-DR) and pointed (contrast-DP) cabbages to be putatively involved in the leafy head formation (Table 1, Fig. S7, B and Table S17). From these 1 998 DEGs, 598 genes were identified only in round cabbage (contrast-DR), 1 072 genes only in pointed cabbage (contrast-DP), and 328 genes in both cabbages (Table 1, Fig. S7, B and Table S17). The MDS dispersion plot of the 17 mRNA libraries based on the expression of these 1 998 DEGs, corrected for genes involved in aging based on collard samples (Fig. S8), confirms that both collard tissue samples (stage-one and -two) cluster close to each other. This is not the case for rosette and heading stage samples from round and pointed cabbages respectively.

To better understand the functions of these 1 998 DEGs, we annotated them using GO terms. In total, 69 GO terms are enriched in these 1 998 DEGs (Table S18). The biological process categories include terms related to lipid, carbohydrate, and cell wall metabolic processes, responses to stress, and signal transduction. The cellular component categories include the terms photosystem, thylakoid, cell wall, and photosynthetic membrane. The molecular function categories include terms related to catalytic activity, DNA-binding transcription factor activity, transcription regulator activity, iron ion binding, and hydrolase activity.

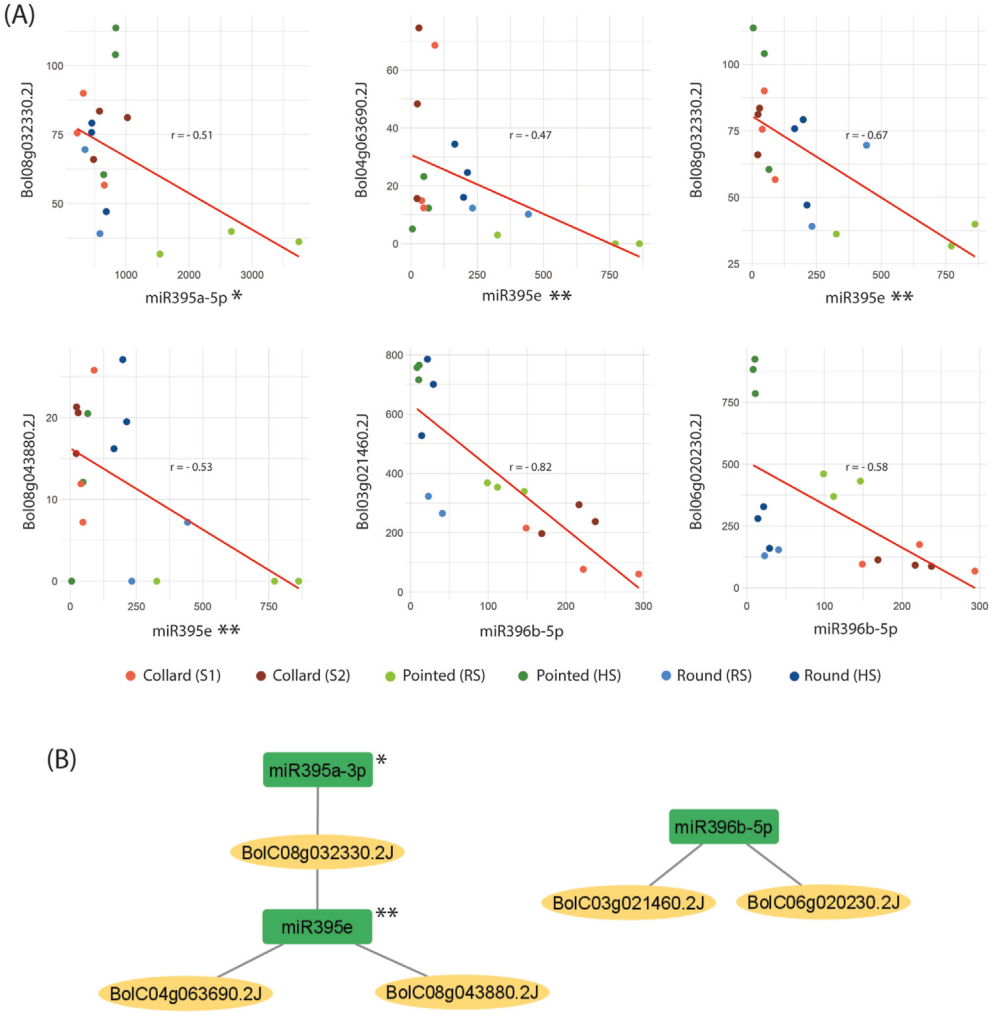

Fig. 5 Integration of differentially expressed miRNAs (DEMs) with differentially expressed genes (DEGs)

A. Scatter plots of the expression of significantly negatively correlated DEMs with DEGs; B. MiRNA-gene regulatory network involved in the leafy head formation in pointed and round cabbage. Green rectangles = DEMs identified with contrast-DP (Development Pointed) in pointed cabbage; yellow ellipses = DEGs identified with contrast-DP in pointed cabbage; *=miR395a/b/c/d; **=miR395e/f. *BolC03g021460.2J* and *BolC06g020230.2J* are *A. thaliana* orthologues of *GRF3* and *GRF4*, respectively.

3.6. Clustering of differentially expressed miRNA-target gene pairs separates cabbage heading leaves from cabbage rosette- and collard leaves

To identify the miRNA-gene interactions with a role in the cabbage leafy head formation, we predicted the target genes of the 33 DEMs putatively involved in the development from the rosette to heading stage of cabbages (contrast-DR and -DP). In total, 773 putative unique miRNA-target gene interactions were identified (Tables S19 and S20). Among these interactions, 33 DEMs are predicted to target 439 (0.74%) of the 59 064 predicted genes from the JZS v2 genome (Cai et al., 2020). Of these 439 target genes, 274 were expressed in at least one of the six leaf tissue samples (Tables S14 and S20) and 39 were identified as DEGs in at least one of the four contrasts that compares the gene abundance of rosette and heading leaves in cabbage (contrast-SR/-SP/-DR/-DP) (Tables S17 and S20). We were especially interested in the miRNA-target gene putative interactions where both transcripts are differentially expressed within the same cabbage morphotype since these should be involved in the leafy head formation process. In total, 37 unique miRNA-target gene predicted interactions were identified where both transcripts (miRNA and gene) are putatively involved in the development from the rosette to heading stage of cabbages (contrast-DR and -DP) (Table S21). From these predicted interactions, 11 were identified in round cabbage with seven DEMs targeting five DEGs and 27 in pointed cabbage with 12 DEMs targeting 14 DEGs. Moreover, one common interaction (miR9408 targeting *BolC06g030010.2J*) was identified in both cabbages. The heatmap with the expression levels of these 18 DEGs predicted to be targets of DEMs (Fig. 4 and Fig. S9) shows that there is moderate consistency between replicates. The heatmap also shows that cabbage (pointed and round) leaf samples collected at heading stage cluster together and dissociate from the cabbage samples collected at rosette stage and both collard samples. Additionally, the two collard samples (stage-one/-two) cluster together.

3.7. Integration of DEMs with DEGs suggest gene regulatory pathways for leafy head formation

To investigate further the 37 unique miRNA-target gene interactions putatively involved in the leafy head formation, we integrated the expression levels of DEMs with the expression of targeted DEGs (among the six morphotype/stage combinations). If a miRNA regulates a predicted targeted gene, we expect to see a negative correlation between the miRNA and gene expression. Indeed, 12 of the 37 miRNA-target gene interactions, including seven miRNAs interacting with five targeted genes, showed such a negative correlation ($P \leq 0.05$, $r < -0.47$; Fig. 5, A) (Table S21). Fig. 5, A visualizes these negative DEMs-DEGs correlations in scatterplots. We are especially interested in plots showing which contrasts between rosette and heading stages in either round or pointed cabbages contributed the most to these overall negative correlations. This was clearly the case for the contrast of the pointed cabbage morphotype with generally low miRNA and high targeted gene transcript levels in heading leaves and vice versa in rosette leaves for miRNA395a-5p, miRNA395e, and miRNA396b-5p (Fig. 5, A). To construct the miRNA-gene regulatory networks that control the leafy head formation in pointed cabbage, the 12 negatively correlated DEM-DEG interaction pairs were analysed with Cytoscape v3.9.1 (Franz et al., 2016). These miRNA-gene regulatory networks highlight the associations of members of the miR395, and miR396 families and their target genes with the leafy head formation process in pointed cabbage (Fig. 5, B). The differentially expressed (DE) miR396b-5p in the pointed cabbage regulates the DE *BolC03g021460.2J* and *BolC06g020230.2J* genes, which are *A. thaliana* orthologues of *GRF3* and *GRF4*, respectively (Table S22).

4. Discussion

4.1. Establishment of developmental stages in cabbage and collard plants

This study aims to identify the miRNA-gene interactions controlling the leafy head formation in round and/or pointed-headed cabbage. We hypothesize that these miRNAs and genes should be differentially expressed between young cabbage leaves that will develop into either flat rosette leaves or curved heading leaves. When comparing these leaves, we expect to identify differentially expressed miRNAs (DEMs) and genes (DEGs) involved in the leafy head formation but also those related to the age (general development) of a *Brassica oleracea* plant, as the rosette stage proceeds the heading stage. To filter the DEMs and DEGs that are involved in the leafy head formation, we removed the miRNAs and genes that were also differentially expressed in young collard leaves that will develop into flat "stage-one" or "stage-two" leaves, which reflect different plant ages, but not developmental stages since they remain flat and do not change their phenotype. Collards were chosen as control as they are closely related to cabbages (Cai et al., 2022), however do not form a leafy head.

In *A. thaliana*, the SPL family of transcription factors is well known to be involved in the plant growth, age, and the transition from juvenile to adult stage (Wu et al., 2006, 2009; Preston and Hileman, 2013). In Chinese cabbage (*B. rapa*), the over-expression of *SPL9-2* accelerated the heading process (Wang et al., 2014), suggesting that *SPL* genes are involved in the leafy head development. However, in a recent study, Zhang et al., (2022) followed the gene expression of young (5 cm) Chinese cabbage leaves in time. In this study, a transition stage was identified between the rosette and heading stages. In order to investigate whether the age pathways (including *SPL* genes) were separate from the developmental pathway, characterized by the transition stage between the rosette and heading stage, they studied the effect of high temperatures. High temperatures delayed the leafy head formation, and timing of the so called transition stage, however the *SPL* expression profiles were not affected, showing that the age pathway is different from the leafy head development pathway. Our study agrees with Zhang et al. (2022) study since no *SPL* genes were identified to be related to the leafy head transition when correcting for age by using collard as a control.

4.2. Analysis of miRNAs

The analysis of the sRNAs identified 111 conserved miRNA molecules, from 43 miRNA families, expressed among the 17

sRNA libraries. From these, miRNA molecules from the miR159, miR162, miR165, miR166, and miR168 families were the most abundant in all leaf tissue samples collected from the three *Brassica* morphotypes. This partially agrees with the results of Lukasik et al. (2013), Wang et al. (2013) and Chen et al. (2022), where miRNA molecules from miR166 and miR168 families were also the most abundant in *Brassica* leaves. The MDS dispersion plot (Fig. 2, C) based on the expression of these 111 conserved miRNAs showed that the round-rosette (tissue from rosette leaves collected from the round cabbages) and pointed-rosette samples cluster together. This was not the case for the round-heading and pointed-heading samples. This suggest that prior to the heading stage, miRNA regulation in both cabbages is relatively similar but diverges starting from the transition into heading stage.

In total, 33 DEMs were identified between rosette and heading leaves of round and pointed cabbages after correction for age (general development) by subtracting the DEMs between stage-one and -two of collard. We hypothesize that these miRNAs have a role in the leafy head formation process. None of these 33 miRNAs were identified in the study of Wang et al. (2013), which compared the miRNA abundances of small leaves (5 mm below the shoot tip) of rosette stage and folding stage plants in Chinese cabbage. The authors do not show data to define what the final destiny of these small leaves will be, whether they will develop into rosette, folding or heading; also the folding stage precedes the leafy head stage. This all complicates a comparison between both studies. Interestingly, some of these 33 DEMs were also found by Chen et al. (2022), who compared miRNA expression in inner and outer leaves of ornamental kale (*Brassica oleracea* L. var. *acephala*). In both our and the Chen's study, miR171b, miR398a-3p, miR6034 and miR9408 were differentially expressed. Ornamental kales are phylogenetically closely related to heading cabbages (Cai et al., 2022) and are semi-heading, forming an open head like structure, like a rose flower. This likely explains these comparable results.

4.3. Analysis of genes

The MDS plot (Fig. S6) of the abundance of > 32 000 genes shows that the overall gene expression separates the three *B. oleracea* morphotypes while the samples of the two developmental stages within the same *B. oleracea* morphotype cluster together. This indicates that the developmental transition from rosette to heading stage in both cabbages and from "stage-one" to "stage-two" in collard is caused by just a fraction of all the expressed genes (Fig. 3). We performed the analysis of DEGs to identify among all the expressed genes the fraction related to the leafy heading process but not the aging in both cabbages morphotypes. This was confirmed by the MDS plot based on the expression of DEGs putatively involved in the leafy head formation (Fig. S8) where collard "stage-one" and "stage-two" leaf tissue samples clustered together while the rosette and heading samples of the same cabbage morphotype separated.

Go enrichment analysis was performed on the genes that are differentially expressed between rosette and heading stages in cabbage but not between "stage-one" and "stage-two" in collard, and therefore possibly involved in leafy head formation. We found enriched GO terms related to DNA-binding transcription factor activity, transcription regulator activity, iron ion binding, photosynthesis, cell wall metabolic processes, response to stress, and signal transduction. These enriched GO terms were also identified in other studies related to the leafy head formation in cabbage (Zhang et al., 2022) and Chinese cabbage (Wang et al., 2012; Sun et al., 2019; Zhang et al., 2022).

4.4. Regulatory network of the leafy head

In this study, we conducted, separately, the analysis of DEMs and DEGs putatively involved in the leafy head formation. To integrate both analyses, we predicted the putative target genes of these DEMs and selected only the subset of target genes identified as DEGs. We found that just a small fraction of the DEGs (18 of 1 998) are predicted to interact with DEMs (18 miRNAs). The heatmap of the expression levels of these DEGs putatively regulated by DEMs (Fig. 4 and Fig. S9) showed that despite the clear variation between biological repeats, samples collected from both cabbage morphotypes at heading stage cluster together and are distinct from the cabbage samples collected a rosette stage and from both collard samples (stage-one and -two). This suggests that these DEGs are associated with the typical heading trait which lacks in the collard control. We also performed a correlation and network analysis with the expression levels of miRNAs and their target genes. Members of the miR395 and miR396 families show participation in the interaction network underlying the leafy head formation in pointed cabbage. Moreover, expression of miR396b-5p is negatively correlated with *BolC03g021460.2J* and *BolC06g020230.2J* genes, which are *B. oleracea* homologues of *Arabidopsis thaliana GROWTH REGULATING FACTORs 3* (*GRF3*) and 4 (*GRF4*) genes. Remarkably, our study did not identify a miRNA-gene interaction related to the leafy head in round cabbage. This can be partially explained by the number of replicates utilized to identify DEMs and DEGs in rosette and heading leaves of round cabbage. We utilized only two of the three replicates of the rosette leaf tissue since one replicate contained a relatively low number of clean reads. This affected the statistical power to identify DEMs and DEGs in round cabbage. Despite this, some of the significant interactions identified in pointed cabbage were almost significant (for BolC06g020230.2J a $\log_2$FC = 0.77, *p*.value = 0.027, and p.adjusted value = 0.150) in round cabbage (Table S23). It is important to note that it may not always be necessary to observe a negative correlation between miRNA expression levels and the expression levels of their target genes in the samples. This is because gene regulation is a complex process involving multiple factors, and the regulating miRNA is just one of these factors influencing the expression of target genes. Additionally, there can be differences in the location where miRNAs are produced, migrate/diffuse and where genes are expressed within the leaf. Several miRNAs are specifically expressed in ad- or abaxial tissues of the leaves (Kalve et al., 2014, Yang et al., 2018); as we sampled complete leaf lamina tissue, we are not able to reveal possible negative correlations between RNA and miRNA across the leaf blade.

The miR396-*GRFs* interaction pair is part of the miR319-*TCPs*-miR396-*GRFs* regulatory network that controls leaf development (Nath et al., 2003; Palatnik et al., 2003; Koyama et al., 2010; Schommer et al., 2014) and cell proliferation (Rodriguez et al., 2010; Sarvepalli and Nath, 2011; Debernardi et al., 2014). In this regulatory network, miR319 (also known as JAW) negatively regulates the expression of *TCP* genes (Palatnik et al., 2003), which represses the expression of cycling genes and controls the final number of cells in

leaves (Schommer et al., 2014). Part of the effects produced by *TCP* genes are mediated by the induction of miR396 (Schommer et al., 2014), which negatively regulates *GRFs* (Rodriguez et al., 2010; Debernardi et al., 2014). GRFs positively regulate cell proliferation and thus the final cell numbers in leaves (Rodriguez et al., 2010).

In Chinese cabbage, the miR319-*TCP4* interaction has been shown to regulate the leafy head shape (Mao et al., 2014). A cylindrical head shape was associated with relatively low *BrpTCP4-1* expression, while a round head shape was associated with high *BrpTCP4-1* expression. The authors concluded that the miR319a-targeted *BrpTCP* gene regulates the round shape of leafy heads via differential cell division arrest in leaf regions. In our study, we showed the miR396-*GRF* interaction to be related to the leafy head shape in pointed cabbage, while this interaction was not significant in round cabbage. The possible involvement of the miR396-*GRF* interaction in the leafy head shape in cabbage should be studied by changing the expression of these transcripts and inspecting the morphology variations produced. It seems that during the convergent domestication in cabbage (*B. oleracea*) and Chinese cabbage (*B. rapa*), the leafy head trait arose through different modifications of the miRNA-gene regulatory networks.

Declaration of interests

The authors declare that they have no known competing financial interests or personal relationships that could have appeared to influence the work reported in this paper.

Acknowledgments

This research was funded by the Mexican government through the Consejo Nacional de Ciencia y Tecnología (CONACYT), C.V. 761325, for the PhD project of Jorge Alemán-Báez. We like to thank staff of Unifarm for taking care of the greenhouse experiments.

Supplementary materials

Supplementary material associated with this article can be found, in the online version, at https://doi.org/10.1016/j.hpj.2023.08.002.

REFERENCES

Allen, E., Xie, Z., Gustafson, A.M., Carrington, J.C., 2005. microRNA-Directed Phasing during Trans-Acting siRNA Biogenesis in Plants. Cell, 121: 207–221.

Benjamini, Y., Hochberg, Y., 1995. Controlling the false discovery rate: a practical and powerful approach to multiple testing. Journal of the Royal Statistical Society: Series B (Methodological), 57: 289–300.

Bolger, A.M., Lohse, M., Usadel, B., 2014. Trimmomatic: a flexible trimmer for Illumina sequence data. Bioinformatics, 30: 2114–2120.

Cai, C., Bucher, J., Bakker, F.T., Bonnema, G., 2022. Evidence for two domestication lineages supporting a middle-eastern origin for *Brassica oleracea* crops from diversified kale populations. Horticulture Research, 9: uhac033.

Cai, X., Wu, J., Liang, J., Lin, R., Zhang, K., Cheng, F., Wang, X., 2020. Improved *Brassica oleracea* JZS assembly reveals significant changing of LTR-RT dynamics in different morphotypes. Theor Appl Genet, 133: 3187–3199.

Chen, C., Chen, H., Zhang, Y., Thomas, H.R., Frank, M.H., He, Y., Xia, R., 2020. TBtools: An integrative toolkit developed for interactive analyses of big biological data. Mol Plant, 13: 1194–1202.

Chen, D., Chen, H., Zhang, H., Dai, G., Shen, W., Liu, Y., Tan, C., 2022. Identification of anthocyanin-related microRNAs in ornamental kale (*Brassica oleracea* L. var. *acephala*) by high throughput sequencing. Scientia Horticulturae, 302: 111153.

Chitwood, D.H., Guo, M., Nogueira, F.T.S., Timmermans, M.C.P., 2007. Establishing leaf polarity: the role of small RNAs and positional signals in the shoot apex. Development, 134: 813–823.

Chitwood, D.H., Nogueira, F.T.S., Howell, M.D., Montgomery, T.A., Carrington, J.C., Timmermans, M.C.P., 2009. Pattern formation via small RNA mobility. Genes Dev, 23: 549–554.

Debernardi, J.M., Mecchia, M.A., Vercruyssen, L., Smaczniak, C., Kaufmann, K., Inze, D., Rodriguez, R.E., Palatnik, J.F., 2014. Post-transcriptional control of *GRF* transcription factors by microRNA miR396 and GIF co-activator affects leaf size and longevity. Plant J, 79: 413–426.

Dong, Q., Hu, B., Zhang, C., 2022. microRNAs and Their Roles in Plant Development. Frontiers in Plant Science, 13. Article 824240.

Enright, A.J., John, B., Gaul, U., Tuschl, T., Sander, C., Marks, D.S., 2003. MicroRNA targets in *Drosophila*. Genome Biology, 5: 2255.

Franz, M., Lopes, C.T., Huck, G., Dong, Y., Sumer, O., Bader, G.D., 2016. Cytoscape.js: a graph theory library for visualisation and analysis. Bioinformatics, 32: 309–311.

Friedländer, M.R., Mackowiak, S.D., Li, N., Chen, W., Rajewsky, N., 2012. miRDeep2 accurately identifies known and hundreds of novel microRNA genes in seven animal clades. Nucleic Acids Res, 40: 37–52.

Gu, A., Meng, C., Chen, Y., Wei, L., Dong, H., Lu, Y., Wang, Y., Chen, X., Zhao, J., Shen, S., 2017. Coupling Seq-BSA and RNA-Seq Analyses Reveal the Molecular Pathway and Genes Associated with Heading Type in Chinese Cabbage. Front Gen, 8: 176.

Islam, W., Idrees, A., Waheed, A., Zeng, F., 2022. Plant responses to drought stress: microRNAs in action. Environmental Research, 215: 114282.

Kim, D., Paggi, J.M., Park, C., Bennett, C., Salzberg, S.L., 2019. Graph-based genome alignment and genotyping with HISAT2 and HISAT-genotype. Nature Biotechnology, 37: 907–915.

Kalve, S., De Vos, D., Beemster, G.T.S., 2014. Leaf development: a cellular perspective. Front Plant Sci, 5: 362.

Kim, J., Jung, J.H., Reyes, J.L., Kim, Y.S., Kim, S.Y., Chung, K.S., Kim, J.A., Lee, M., Lee, Y., Kim, V.N., Chua, N., Park, C., 2005. microRNA-directed cleavage of *ATHB15* mRNA regulates vascular development in *Arabidopsis* inflorescence stems. Plant J, 42: 84–94.

Knauer, S., Holt, Anna L., Rubio-Somoza, I., Tucker, E.J., Hinze, A., Pisch, M., Javelle, M., Timmermans, M.C., Tucker, M.R., Laux, T., 2013. A protodermal miR394 signal defines a region of stem cell competence in the *Arabidopsis* shoot meristem. Developmental Cell, 24: 125–132.

Koyama, T., Mitsuda, N., Seki, M., Shinozaki, K., Ohme-Takagi, M., 2010. TCP transcription factors regulate the activities of ASYMMETRIC LEAVES1 and miR164, as well as the auxin response, during differentiation of leaves in *Arabidopsis*. Plant Cell, 22: 3574–3588.

Kumar, K., Mandal, S.N., Neelam, K., de los Reyes, B.G., 2022. MicroRNA-mediated host defense mechanisms against pathogens and herbivores in rice: balancing gains from genetic resistance with trade-offs to productivity potential. BMC Plant Biology, 22: 351.

Langmead, B., Salzberg, S.L., 2012. Fast gapped-read alignment with Bowtie 2. Nature Methods, 9: 357–359.

Li, J., Zhang, X., Lu, Y., Feng, D., Gu, A., Wang, S., Wu, F., Su, X., Chen, X., Li, X., Liu, M., Fan, S., Feng, D., Luo, S., Xuan, S., Wang, Y., Shen, S., Zhao, J., 2019. Characterization of Non-heading Mutation in Heading Chinese Cabbage (*Brassica rapa* L. ssp. *pekinensis*). Front Plant Sci, 10: 112.

Liu, Z., Jia, L., Wang, H., He, Y., 2011. HYL1 regulates the balance between adaxial and abaxial identity for leaf flattening via miRNA-mediated pathways. J Exp Bot, 62: 4367–4381.
Lukasik, A., Pietrykowska, H., Paczek, L., Szweykowska-Kulinska, Z., Zielenkiewicz, P., 2013. High-throughput sequencing identification of novel and conserved miRNAs in the *Brassica oleracea* leaves. BMC Genomics, 14: 801.
Mao, Y., Wu, F., Yu, X., Bai, J., Zhong, W., He, Y., 2014. microRNA319a-targeted *Brassica rapa* ssp. *pekinensis TCP* genes modulate head shape in Chinese cabbage by differential cell division arrest in leaf regions. Plant Physiology, 164: 710–720.
Nath, U., Crawford, B.C.W., Carpenter, R., Coen, E., 2003. Genetic Control of Surface Curvature. Science, 299: 1404–1407.
Nawrocki, E.P., Eddy, S.R., 2013. Infernal 1.1: 100-fold faster RNA homology searches. Bioinformatics, 29: 2933–2935.
Palatnik, J.F., Allen, E., Wu, X., Schommer, C., Schwab, R., Carrington, J.C., Weigel, D., 2003. Control of leaf morphogenesis by microRNAs. Nature, 425: 257–263.
Pertea, M., Pertea, G.M., Antonescu, C.M., Chang, T.C., Mendell, J.T., Salzberg, S.L., 2015. StringTie enables improved reconstruction of a transcriptome from RNA-seq reads. Nature Biotechnology, 33: 290–295.
Preston, J., Hileman, L., 2013. Functional evolution in the plant *SQUAMOSA-PROMOTER BINDING PROTEIN-LIKE (SPL)* Gene Family. Front Plant Sci, 4: 80.
R Core Team, 2022. "R: A language and environment for statistical computing.", (ed.) R.F.f.S. Computing. https://www.R-project.org/
Raman, S., Greb, T., Peaucelle, A., Blein, T., Laufs, P., Theres, K., 2008. Interplay of miR164, *CUP-SHAPED COTYLEDON* genes and *LATERAL SUPPRESSOR* controls axillary meristem formation in *Arabidopsis thaliana*. Plant J, 55: 65–76.
Rehmsmeier, M., Steffen, P., Hochsmann, M., Giegerich, R., 2004. Fast and effective prediction of microRNA/target duplexes. RNA, 10: 1507–1517.
Ren, W., Wang, H., Bai, J., Wu, F., He, Y., 2018. Association of microRNAs with Types of Leaf Curvature in *Brassica rapa*. Front Plant Sci, 9: 73.
Ritchie, M.E., Phipson, B., Wu, D., Hu, Y., Law, C.W., Shi, W., Smyth, G.K., 2015. limma powers differential expression analyses for RNA-sequencing and microarray studies. Nucleic Acids Res, 43: e47.
Robinson, M.D., McCarthy, D.J., Smyth, G.K., 2010. edgeR: a Bioconductor package for differential expression analysis of digital gene expression data. Bioinformatics, 26: 139–140.
Robinson, M.D., Oshlack, A., 2010. A scaling normalization method for differential expression analysis of RNA-seq data. Genome Biology, 11: R25.
Rodriguez, R.E., Mecchia, M.A., Debernardi, J.M., Schommer, C., Weigel, D., Palatnik, J.F., 2010. Control of cell proliferation in *Arabidopsis thaliana* by microRNA miR396. Development, 137: 103–112.
Sarvepalli, K., Nath, U., 2011. Hyper-activation of the TCP4 transcription factor in *Arabidopsis thaliana* accelerates multiple aspects of plant maturation. Plant J, 67: 595–607.
Schneider, C.A., Rasband, W.S., Eliceiri, K.W., 2012. NIH Image to ImageJ: 25 years of image analysis. Nature Methods, 9: 671–675.
Schommer, C., Debernardi, J.M., Bresso, E.G., Rodriguez, R.E., Palatnik, J.F., 2014. Repression of cell proliferation by miR319-regulated TCP4. Mol Plant, 7: 1533–1544.
Sha, Y., Phan, J.H., Wang, M.D., 2015. Effect of low-expression gene filtering on detection of differentially expressed genes in RNA-seq data. Annu Int Conf IEEE Eng Med Biol Soc 6461–6464.
Shen, W., Le, S., Li, Y., Hu, F., 2016. SeqKit: A Cross-Platform and Ultrafast Toolkit for FASTA/Q File Manipulation. PLOS ONE, 11: e0163962.
Song, J.B., Huang, S.Q., Dalmay, T., Yang, Z.M., 2012. Regulation of leaf morphology by microRNA394 and its target LEAF CURLING RESPONSIVENESS. Plant Cell Physiol, 53: 1283–1294.
Sun, X., Basnet, R.K., Yan, Z., Bucher, J., Cai, C., Zhao, J., Bonnema, G., 2019. Genome-wide transcriptome analysis reveals molecular pathways involved in leafy head formation of Chinese cabbage (*Brassica rapa*). Horticulture Research, 6: 130.
Wang, F., Li, L., Li, H., Liu, L., Zhang, Y., Gao, J., Wang, X., 2012. Transcriptome analysis of rosette and folding leaves in Chinese cabbage using high-throughput RNA sequencing. Genomics, 99: 299–307.
Wang, F., Li, L., Liu, L., Li, H., Zhang, Y., Yao, Y., Ni, Z., Gao, J., 2012b. High-throughput sequencing discovery of conserved and novel microRNAs in Chinese cabbage (*Brassica rapa* L. ssp. *pekinensis*). Molecular Genetics and Genomics, 287: 555–563.
Wang, F., Li, H., Zhang, Y., Li, J., Li, L., Liu, L., Wang, L., Wang, C., Gao, J., 2013. MicroRNA expression analysis of rosette and folding leaves in Chinese cabbage using high-throughput Solexa sequencing. Gene, 532: 222–229.
Wang, Y., Wu, F., Bai, J., He, Y., 2014. *BrpSPL9* (*Brassica rapa* ssp. *pekinensis SPL9*) controls the earliness of heading time in Chinese cabbage. Plant Biotechnology J, 12: 312–321.
Wickham, H., 2016. ggplot2: elegant graphics for data analysis. Springer-Verlag, New York.
Williams, L., Grigg, S.P., Xie, M., Christensen, S., Fletcher, J.C., 2005. Regulation of *Arabidopsis* shoot apical meristem and lateral organ formation by microRNA *miR166g* and its *AtHD-ZIP* target genes. Development, 132: 3657–3668.
Wu, G., Park, M.Y., Conway, S.R., Wang, J.-W., Weigel, D., Poethig, R.S., 2009. The sequential action of miR156 and miR172 regulates developmental timing in *Arabidopsis*. Cell, 138: 750–759.
Wu, G., Poethig, R.S., 2006. Temporal regulation of shoot development in *Arabidopsis thaliana* by *miR156* and its target *SPL3*. Development, 133: 3539–3547.
Yamaguchi, T., Nukazuka, A., Tsukaya, H., 2012. Leaf adaxial-abaxial polarity specification and lamina outgrowth: evolution and development. Plant Cell Physiol, 53: 1180–1194.
Yang, T., Wang, Y., Teotia, S., Zhang, Z., Tang, G., 2018. The making of leaves: How small RNA networks modulate leaf development. Front Plant Sci, 9: 824.
Ye, B., Wang, R., Wang, J., 2016. Correlation analysis of the mRNA and miRNA expression profiles in the nascent synthetic allotetraploid *Raphanobrassica*. Scientific Reports, 6: 37416.
Zhang, B., Pan, X., Cannon, C.H., Cobb, G.P., Anderson, T.A., 2006. Conservation and divergence of plant microRNA genes. Plant J, 46: 243–259.
Zhang, L.B., Xia, H., Wu, J.S., Li, M.T., 2022. MiRNA identification, characterization and integrated network analysis for flavonoid biosynthesis in *Brassicacoraphanus*. Hortic Plant J, 8: 319–327.
Zhang, K., Yang, Y., Wu, J., Liang, J., Chen, S., Zhang, L., Lv, H., Yin, X., Zhang, X., Zhang, Y., Zhang, L., Zhang, Y., Freeling, M., Wang, X., Cheng, F., 2022. A cluster of transcripts identifies a transition stage initiating leafy head growth in heading morphotypes of *Brassica*. Plant J, 110: 688–706.
Zhang, Y., Verbeek, F., 2010. Comparison and Integration of Target Prediction Algorithms for microRNA Studies. Journal of Integrative Bioinformatics, 7: 3.
Zhu, W., Zhang, M., Li, J., Zhao, H., Zhang, K., Ge, W., 2022. Key regulatory pathways, microRNAs, and target genes participate in adventitious root formation of *Acer rubrum* L. Scientific Reports, 12: 12057.